

Forecast of Mine Inflow using In-situ Well Test and Visual Modflow in an Underground Mine

Myong Song Song, Kun Ui Hong

Faculty of Mining Engineering, Kim Chaek University of Technology, Pyongyang, Democratic People's Republic of Korea

Un Chol Han (corresponding author)

School of Science and Engineering, Kim Chaek University of Technology, Pyongyang, Democratic People's Republic of Korea

Il Yong Kang

School of Science and Engineering, Kim Chaek University of Technology, Pyongyang, Democratic People's Republic of Korea

Yong Il Ri

Faculty of Anthracite Mining Engineering, Pyong Song University of Coal Mining, Pyongsong, Democratic People's Republic of Korea

ABSTRACT: Water inrush in mining field is considered as one of the major dangerous factors for production safety and worker's life in coal mines. In this paper for underwater flow, repeat measurements of water level is essential to water inrush forecasting, so the control point drawdown must be clearly calculated in accordance with the mining construction plans, dewatering period and drainage time. We determined optimal parameters in relation to the water inrush forecasting using the PEST-ASP module in Visual MODFLOW in order to get accurately the groundwater flow distribution at the control points, including normal and maximum water inrush. Comparing simulation results and in-situ data of water inrush, the relative error was lower than 0.74%, showing that this method is the most reasonable one for forecasting water inrush in a coal mine.

Keywords: Numerical Simulation, water Inrush, Visual MODFLOW, Pumping well.

1 INTRODUCTION

As human activities and climate change are becoming more and more intensive, groundwater problems such as groundwater pollution and water shortage are getting worse and worse. Numerical simulation, a useful tool for groundwater management and protection, is always used for solving these problems. In-depth understanding of groundwater system characteristics and can be reached with the mathematical model (Bukowski 2011).

Dumpleton et al. (2001) used 3-D visualization and predictive modeling to evaluate the risk of mine water inrush in mine. Hodlur et al. (2002) proposed a statistical hydrogeological model to evaluate water inrush risk.

The dynamic changes of climate and human activities have altered the natural flow of rivers (Gädeke et al. 2014; Li et al. 2014) and in some arid and semiarid regions, flow of many rivers continues to decrease, even appeared zero flow in dry season. Zhang (2005) presented the water inrush mechanism and applied the finite element method coupled with stress-dependent permeability to predict water inrush, proposing some technical measures to improve mine design and safety. Kong et al. (2007) used a theory of seepage instability to estimate the harmfulness of water inrush from an ore seam roof in a particular mine of the Mining Group. Han J (2019)

presented the methods of strata mechanics and finite element analysis to describe the mechanism of mine water inrush through a fault from the roof. Bukowski (2011) proposed a risk assessment system to analyze water hazard, based on the factors of inflow intensity, the amount of suspended material contained in the water flowing into mine water, the proportion of water-bearing formations in the vertical profile, the condition of the shaft lining and safety pillar, and life of the shaft. Chen & Yang (2011) applied Fault Tree Analysis (FTA) to analyze the hazard common source of mine water inrush.

The groundwater flow problems and the water inrush estimation problems can be solved efficiently by numerical simulation. In order to correctly calculate the water inrush in Sanbin Mine and the numerical simulation method is used to establish a three-dimensional numerical simulation model with Visual MODFLOW. The optimal parameters for simulating the groundwater flow can be determined with win-PEST of Visual MODFLOW.

Sanbin Mine is located in the western of Win River in the southern of Sariwon city. The main topographies in the study area are covered with sand, sandy gravel and lime stone and valley terrace. The groundwater type is mainly Quaternary loose rock pore phreatic water and Cretaceous rock fissure-pore water. The Cretaceous classic rock fissure-pore water spreads all over the study area and surface water flows through the fracture.

2 FORECAST METHOD

2.1 Conceptual model

A Conceptual Model refers to a basic, high-level representation of the hydrogeological system is modeled. It will form the foundation for one or more numerical models. In Visual MODFLOW, the conceptual model is completely grid and simulator independent. This means you define the inputs using your raw data objects (surfaces, polylines, polygons, etc.). The grid or mesh is only introduced at the time of launching a numerical model. This allows you to:

Convert the conceptual model to multiple numerical models for uncertainty analysis.

Convert the conceptual model to a MODFLOW or FEFLOW model

Easily update corresponding numerical models as your conceptualization changes

Basically, a groundwater model is a simplified representation of the natural groundwater flow system. Without them it would be impossible to evaluate all of the natural processes that impact a hydro-geologic design because of complexities in

- The physical processes that occur in the hydro-geologic environment,
- The spatial distribution of properties and boundaries,
- The temporal nature of the flow system

The middle part of the western boundary receives lateral runoff supply and can be conceptualized as flow boundary. Sanbin River, located in the south of the study area, can be conceptualized as constant head boundary. Other surrounding boundaries can be seen as confining ones. The lower interface is conceptualized as confining boundary.

2.2 Numerical model

The following three-dimensional transient flow numerical model is set up based on the above hydrogeological conceptual model (Hodlur, G., Prakash, R.M., Deshmukh, S. & Singh, V. 2002):

$$\frac{\partial}{\partial x}(K_{xx} \frac{\partial h}{\partial x}) + \frac{\partial}{\partial y}(K_{yy} \frac{\partial h}{\partial y}) + \frac{\partial}{\partial z}(K_{zz} \frac{\partial h}{\partial z}) - W = S_s \frac{\partial h}{\partial t} \quad (1)$$

where K_{xx} , K_{yy} , K_{zz} -hydraulic conductivity to x, y, z orientation separately (m/d); h -water head (m); S_s -storage coefficient of the aquifer under the water table (1/m); μ -specific yield; W is the precipitation recharge intensity.

It can be classified as follows according to the properties. First boundary condition, Second boundary condition, transient flow boundary (constant boundary condition).

Hydraulic conductivity, porosity of rock, storage coefficient of the aquifer, diffusion coefficient parameters need to be identified.

3 FORECAST OF WATER INRUSH BY VISUAL MOFLOW

The correct drainage method according to normal mining in colliery depends on the atmospheric precipitation, so we must determine the water level on every point. We should estimate the overflow quantities when water level on every point goes down until required water level.

The normal water inrush is the average of annual quantities, maximum water inrush are the max precipitation, which is the water inrush determined under max water level condition.

3.1 *Building of groundwater model*

3.1.1 *Building of area boundary condition*

The natural geological boundary range is F14 fault in the East, F21 fault in the West, F21 fault in the North, and F15 fault in the South. In this paper, the area of study zone is 23km², with the east-west length of 5.4km, and the south-north length of 4.5km.

In 3D space, the entire study area is discretized by a 90m×70m grid paralleling to x and y into 10 800 cells (6 012 active cells, 4 788 in-active cells), there are three layers vertically, so the total active cells are 12 024 (see Figure 1).

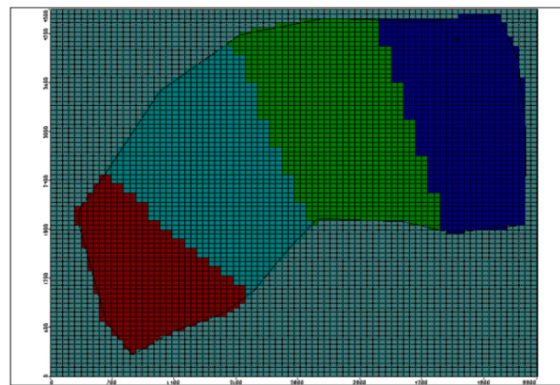


Figure 1. The first layer of aquifer parameters zoning map.

3.1.2 *Hydro-geologic parameters zone*

The study area has 18 observation wells in all, 5 supplementary observation wells of them are measurement wells. In this paper the flow property using the pumping testing data on each observation well is simulated. The hydraulic conductivity was determined using the pumping test data, dividing the simulation area into 9 parameter zones according to the geological conditions, such as the property of rock and water level. The first layer includes 4 areas and the second layer is the coal layer that includes one area. The third layer is aquifer, which divides by 4 areas, the hydraulic conductivity in each area is decided by hydrogeologic condition and hydraulic conductivity of any cell in groundwater model.

In the paper, we determined the hydraulic conductivity similar to actual value using PEST module of Visual MODFLOW. It shows the first layer of aquifer parameters zoning map, zoning map of Seam parameters respectively and second layer of aquifer parameters zoning map in Figure 1.

3.2 *Model Calibration and Verification*

We calibrated and verified the parameters using PEST module of Visual MODFLOW. The parameter optimization of PEST-ASP process is shown in Figure 2. We can modify the hydrogeologic parameters using Visual MODFLOW/Win PEST in order to approach to real value.

The hydraulic conductivity of 9 optimization parameters can be optimized selecting “log” button in optimization selecting item of PEST control window. We used the water level values at 10 pumping wells as observation data. The results showed at Table 1.

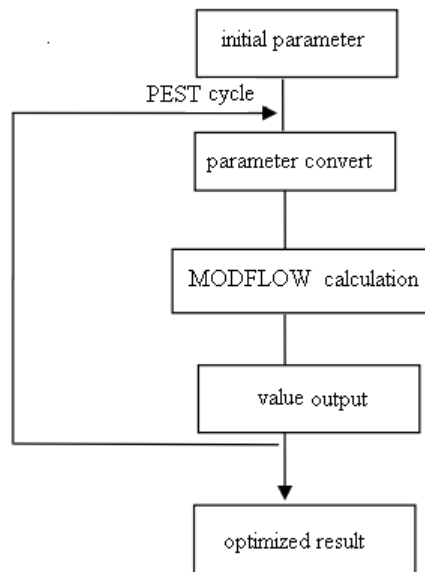


Figure 2. Parameter optimization of PEST -ASP processes.

Table 1. Calibrated parameters using PEST optimization process.

Area name	Kx, m/s	Ky, m/s	Kz, m/s
01	1.58E-6	1.89E-6	2.22E-7
02	8.89E-7	1.25E-6	1.94E-7
03	1.94E-6	2.5E-6	3.06E-7
04	2.78E-6	2.33E-6	4.17E-7
05	7.07E-7	6.08E-7	2.14E-7
06	1.79E-6	2.34E-6	1.33E-7
07	2.29E-6	3.59E-6	2.03E-7
08	2.48E-6	2.99E-6	1.98E-7
09	3.04E-6	2.91E-6	2.46E-7

Based on the pumping data of observation well in study area and using the optimized parameters such as hydrogeologic conductivity, porosity and so on, we determined the fit flow field of groundwater as shown in Figure 3. As you can see in Figure 3, the highest water level is 38m and lowest water level is 32m.

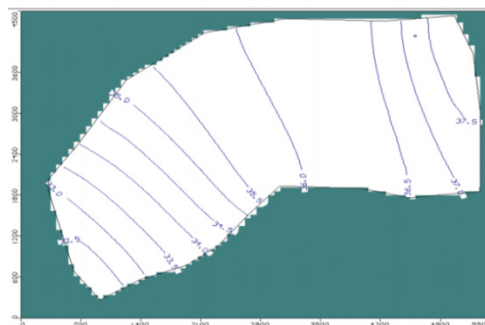


Figure 3. Fit flow field.

In order to ensure the simulated result we must modify groundwater flow model correctly. In order words, we must consider all well as observation well and compare the simulation result with actual data. Then it calculates the error between the initial water level and deviation fitting water level in every borehole. (See Table 2)

Table 2. Deviation of fitting.

No	Initial level, m	Deviation of fitting, m	Error, %	No	Initial level, m	Deviation of fitting, m	Error, %
G-67	32.4	32.7	0.93	P-2	33.8	33.4	1.2
X-3	32.3	32.6	0.88	X-11	35.0	34.5	1.7
P-6	36.1	35.0	2.6	P-10	36.3	35.6	2.0
P-1	36.0	36.0	2.5	P-3	37.8	37.5	0.8
P-9	36.4	36.0	1.1	P-5	36.3	35.6	2.0
P-11	36.5	35.3	3.3	P-4	36.6	34.8	4.9
P-13	36.2	34.7	4.1	X-4	32.1	33.8	5.3

As it can see in table, the deviation of fitting in 10 boreholes was below 3 percent and accounted for 71.4 percent. The deviation of fitting 3 boreholes were from 3 to 5 percent and accounted for 21.4 percent, the deviation of fitting one borehole(X-4 borehole) was more than 5 percent and accounted for 7.2 percent.. As shown above, we recognized that table fitting deviation existed within limit extent and selection of model parameters is reasonable. Thus, it can simulate the water inrush under various conditions in-site by this model.

3.3 Forecasting plan for simulation

Water inrush forecast problem is the one that solve the groundwater flow state based on the reversible change such as state change in study area. We used Visual MODFLOW/WHM solver, which uses a Bi-Conjugate Gradient Stabilized (Bi-CGSTAB) acceleration routine implemented with Stone incomplete decomposition for preconditioning of the groundwater flow partial differential equations. This solver, as all iterative solvers, approaches the solution of a large set of partial differential equations iteratively through an approximate solution. Because the matrix equation for groundwater flow is initially "ill-conditioned", effective preconditioning of these matrices is necessary for an efficient solution. According to the hydrogeologic condition, geotechnologic condition and mining state in study area, we selected 3 forecasting plans for simulation, that is, flow field under natural exploitation in 1 years, flow field under natural exploitation in 2 years and flow field under natural exploitation in 3 years.

It showed the flux at each period in Table 3 based on the forecasting plans finally.

Table 3. Forecast flow at each time under natural condition (m³/h).

Year	Jan	Feb	Mar	Apr	May	Jun	Jul	Aug	Sep	Oct	Nov	Dec
1	308	306	324	337	343	356	379	391	397	362	342	317
2	322	327	326	342	347	353	372	389	396	373	363	332
3	324	319	330	339	351	360	382	396	403	378	359	338

As shown in Table 3, flux under natural exploitation is an average of 346.8m³/h and maximum of 397 m³/h in 1 years, average 354.3 m³/h and maximum of 396 m³/h in 2 years, and average of 356 m³/h and maximum of 403 m³/h in 3 years.

3.4 Indication verification of model

In this paper, we analyzed the hydro-geologic condition and determined boundary and water supply condition, then conceptualized the model.

The numerical model using Visual MODFLOW and optimized parameters by Win-PEST coincided with actual condition.

4 CONCLUSIONS

In this paper, we simulated the water flow distribution state considering the hydrogeological conditions and detailed data in accordance with pumping well tests of the mine.

(1) The Visual MODFLOW software was adopted to simulate the groundwater flow in Sanbin River water source. By model calibration and verification, the simulation results and the measured results are in good agreement, and it can be applied to predict the water flow under future mining conditions.

(2) On the basis of simulation prediction, the water level in 14 observation boreholes is comparative analyzed. Deviation of fitting 10 observation boreholes was below 3 percent. From this, we can determine the flux at every borehole under 3 natural exploitation forecast plan. Result of comparative analysis between the simulation data and actual data, the deviation was less than 0.74 percent. Thus, it is considered to be optimal parameters in which both the local ecological environment and the Sanbin River flow is influenced to coal mining.

ACKNOWLEDGEMENTS

The authors gratefully acknowledge the financial support from the National Science and Technical Development Foundation of DPR Korea (Grant No. 24)

REFERENCES

- Bukowski, P. 2011. Water hazard assessment in active shafts in upper Silesian coal basin mines. *Mine Water Environ* 30, pp. 302–11.
- Chen, J.M. & Yang, R.S. 2011. Analysis of mine water inrush accident based on FTA. *Proc Environ Sci* 11 pp. 1550–1554.
- Dumpleton, S., Robins. N.S., Walker, J.A. & Merrin, P.D. 2011. Mine water rebound in south Nottinghamshire: risk evaluation using 3-D visualization and predictive modeling. *Q J Eng Geol Hydrogeol* 34 (3), pp. 307–319.
- Gädeke, A., Hölzel, H., Koch, H., Pohle, I., Grünewald, U., 2014. Analysis of uncertainties in the hydrological response of a model-based climate change impact assessment in a subcatchment of the Spree River, Germany. *Hydrol. Process.* 28, 3978–3998.
- Han, J., Shi. L.Q., Yu, X.G., 2019. Mechanism of mine water-inrush through a fault from the roof. *Min Sci Tech* 19, pp. 276–281.
- Hodlur, G., Prakash, R.M., Deshmukh, S. & Singh, V. 2002. Role of some salient geophysical, geochemical, and hydrogeological parameters in the exploration of fresh groundwater in a brackish terrain. *Environ Geol* 41 (7), pp. 861–866
- Kong, H.L., Miao, X.X., Wang, L.Z, 2007. Analysis of the harmfulness of water inrush from ore seam roof based on seepage instability theory. *J China Univ Min Tech* 17 (4), pp. 453–458.
- Li, F., Zhang, G., Xu, Y.J., 2014. Spatiotemporal variability of climate and streamflow in the Songhua River Basin, northeast China. *J. Hydrol.* 514, 53–64
- Zhang, J. 2005. Investigations of water inrushes from aquifers under ore seams. *Int J Rock Mech Min Sci* 42, pp. 350–360.